Int. J. Solids Structures Vol. 20, No. 1, pp. 81–91, 1984
Printed in Great Britain.

0020-7683/84 $3.00 + .00
Pergamon Press Ltd.

QUASI-STATIC NORMAL INDENTATION OF AN ELASTO–PLASTIC HALF-SPACE BY A RIGID SPHERE—I

ANALYSIS

P. S. FOLLANSBEE
Group CMB-5 MS 730, Los Alamos National Laboratories, Los Alamos, NM 87545, U.S.A.

and

G. B. SINCLAIR
Department of Mechanical Engineering, Carnegie-Mellon University, Pittsburgh, PA 15213, U.S.A.

(*Received* 4 *February* 1982; *in revised form* 18 *April* 1983)

Abstract—The title problem is treated, under the conditions of frictionless and completely adhesive contact, within the context of incremental elasto–plasticity. The analysis employs a constant-strain-triangle, finite element code, together with a new grid expansion technique which aids computational efficiency. Preliminary results are presented and compared with the classical elastic solution for the first load step and with a set of experimental results for subsequent load steps; these comparisons demonstrate that the approach has the necessary resolution to reliably determine further results of physical importance.

INTRODUCTION

Contact problems concern the determination of the responses induced in two solids when they are pressed together. Such problems occur often in engineering so that the literature is rich in related investigations; Kalker[1] gives a general review through 1977.

The contact problem of interest here concerns the stresses and deformations that accumulate when a sphere is slowly pressed normally into a relatively soft half-space. This configuration most closely reflects the physical situation encountered in the Brinell hardness test, a procedure for estimating the hardness of materials appealing to metallurgists in its simplicity (a good description of hardness testing may be found in [2], Chap. 11). The configuration in addition has implications for the effects of ball bearings on bearing races as discussed by Tyler, Burton and Ku[3], and can be used to aid understanding of the mechanisms involved in particulate erosion at sufficiently low speeds as in Follansbee, Sinclair and Williams[4]. To a lesser extent because of the impact speeds involved, this last use can also be applied to shot-peening operations (see, e.g. Almen and Black[5], Chap. 6 for specifics of such prestressing). In all, this contact problem is of some significance in engineering.

There have been quite a number of studies made of the problem dating back over the last century; Tabor's book [6], though somewhat out-of-date now, remains an outstanding commentary and Johnson[7] provides an insightful review to 1982. Probably the earliest contribution is Hertz's classical elastostatic solution [8] for the frictionless normal contact of two spheres, one of which can be taken in the limit as a half-space. In many practical cases, however, the indentation is such that yielding occurs in the substrate, limiting the value of .his elastic solution.† One of the first attempts to incorporate plastic flow is the slip-line treatment furnished by Ishlinsky[9] (see also Tabor[6], Chap. 4). While the extension of slip-line theory for plane geometries to the axisymmetric instance has since been justified by Shield[10], the absence of any elastic deformations whatsoever makes it impossible to track the responses as they proceed from purely elastic to predominantly plastic using this theory. One means of overcoming this shortcoming is to use the theory

†Indeed, in an experiment described subsequently in this paper, yielding first occurs when a hard spherical indenter of diameter 1/16 in. (1.59 mm) is pressed into a steel surface with a load as small as 10^{-3} lbf (4×10^{-3} N).

of incremental elasto–plasticity which includes both elastic and plastic deformations and has the further attribute of admitting strain-hardening. Unfortunately these improvements are at the expense of tractability so that attempts reported to analyze the problem within this theory are numerical, for the most part using the finite element method; see Hardy, Baronet and Tordion[11], Lee, Masaki and Kobayaschi[12] and the references contained therein. Even with recourse to numerical methods the problem resists solution: Hardy *et al.*[11] use a fine finite element grid which captures the critical field quantities with sufficient resolution but, because of the attendant computational effort, severely limits the extent to which the half-space can be loaded in excess of elastic; Lee *et al.*[12] on the other hand take the loading forward to the higher levels experienced in practice but in so doing sacrifice the resolution of a fine grid, thereby introducing a considerable amount of numerical noise into their results. What we seek to do here is to treat the problem within incremental elasto–plasticity with a finite element grid of sufficient resolution and accuracy, yet to take the calculations through to the point of including the upper load levels normally encountered in applications.

In meeting our objective we are aided by a new generation of computers since [11, 12] and by a straightforward but efficient expansion technique for the finite element method: this last maintains resolution comparable to that of Hardy *et al.* [11] while reducing computation times by about an order of magnitude. Together these advances enhance computational capability sufficiently to enable calculations to be carried forward to higher loads assuming frictionless and completely adhesive contact, thereby bounding the effects of friction. Nonetheless, the approach still entails a significant computational effort, one that other analysts may well not welcome redoing in order to obtain specific information of interest to them. Accordingly we attempt to furnish as comprehensive a set of results as possible in a second paper; here we describe the method of analysis and those results which allow an evaluation of its reliability.

We begin in Section 1 by formulating the class of problems considered, then describe how the analysis is carried out in Section 2. Finally, in Section 3 we present selected results and an experimental comparison with a view to validating the approach.

1. FORMULATION

Here we set down a class of problems which addresses the determination of the stresses, strains and displacements that accumulate in an initially undisturbed, elasto-plastic, half-space when a rigid sphere is slowly pressed normally into its surface.

To this end let (x, y, z) be rectangular cartesian coordinates with origin O such that the surface of the half-space $\mathscr{H}$ is formed by the xy-plane with z positive into $\mathscr{H}$ (Fig. 1). Further let (r, θ, z) be cylindrical polar coordinates related to the rectangular coordinates by

$$x = r\cos\theta,\ y = r\sin\theta,\ z = z\ (0 \le r < \infty,\ 0 \le \theta < 2\pi,\ -\infty < z < \infty). \tag{1.1}$$

Thus

$$\mathscr{H} = \{(r, \theta, z) | 0 \le r < \infty,\ 0 \le \theta < 2\pi,\ 0 < z < \infty\}. \tag{1.2}$$

At some time $t > 0$, a rigid sphere of radius R indents the half-space under load P to the extent that contact occurs on a circle centered on O with radius a. That is, if $\partial_1\mathscr{H}$ is the contact region and $\partial_2\mathscr{H}$ the half-space surface free from contact, we have

$$\begin{aligned} \partial_1\mathscr{H} &= \{(r, \theta, z) | 0 \le r < a,\quad 0 \le \theta < 2\pi,\ z = 0\}, \\ \partial_2\mathscr{H} &= \{(r, \theta, z) | a < r < \infty,\ 0 \le \theta < 2\pi,\ z = 0\}. \end{aligned} \tag{1.3}$$

We seek then, the *axisymmetric* stresses $\sigma = (\sigma_r, \sigma_\theta, \sigma_z, \tau_{rz})$, strains $\epsilon = (\epsilon_r, \epsilon_\theta, \epsilon_z, \gamma_{rz})$ and displacements $u = (u, w)$, as functions of r, z throughout $\mathscr{H}$ for all time $t > 0$, resulting from the accumulation of their corresponding rates in accordance with

$$\sigma = \int_0^t \dot{\sigma}\,\mathrm{d}t,\ \epsilon = \int_0^t \dot{\epsilon}\,\mathrm{d}t,\ u = \int_0^t \dot{u}\,\mathrm{d}t, \tag{1.4}$$

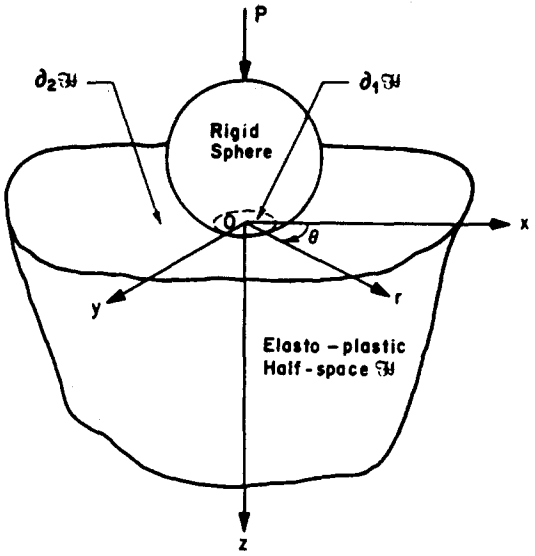

Fig. 1. Geometry and coordinates for the indented half-space

on $\mathscr{H}$, wherein the rate quantities $\dot{\sigma} = (\dot{\sigma}_r, \dot{\sigma}_\theta, \dot{\sigma}_z, \dot{\tau}_{rz})$, $\dot{\epsilon} = (\dot{\epsilon}_r, \dot{\epsilon}_\theta, \dot{\epsilon}_z, \dot{\gamma}_{rz})$, $\dot{u} = (\dot{u}, \dot{w})$ are to satisfy the following requirements.† The axisymmetric, stress-rate, *equations of equilibrium*, in the absence of body forces under the assumption of quasi-static response,

$$\frac{\partial \dot{\sigma}_r}{\partial r} + \frac{\partial \dot{\tau}_{rz}}{\partial z} + \frac{\dot{\sigma}_r - \dot{\sigma}_\theta}{r} = 0,$$
$$\frac{\partial \dot{\sigma}_z}{\partial z} + \frac{\partial \dot{\tau}_{rz}}{\partial r} + \frac{\dot{\tau}_{rz}}{r} = 0, \tag{1.5}$$

on $\mathscr{H}$ for $t > 0$. The *flow rule* for a homogeneous and isotropic, elastic/incompressible-plastic solid complying with von Mises' yield criterion and Drucker's hypothesis,

$$\begin{aligned}
\dot{\sigma}_r &= 2\mu[((\alpha+1) - \beta s_r^2)\dot{\epsilon}_r + (\alpha - \beta s_r s_\theta)\dot{\epsilon}_\theta + (\alpha - \beta s_r s_\zeta)\dot{\epsilon}_z - \beta s_r s_{rz}\dot{\gamma}_{rz}],\\
\dot{\sigma}_\theta &= 2\mu[(\alpha - \beta s_\theta s_r)\dot{\epsilon}_r + ((\alpha+1) - \beta s_\theta^2)\dot{\epsilon}_\theta + (\alpha - \beta s_\theta s_z)\dot{\epsilon}_z - \beta s_\theta s_{rz}\dot{\gamma}_{rz}],\\
\dot{\sigma}_z &= 2\mu[(\alpha - \beta s_z s_r)\dot{\epsilon}_r + (\alpha - \beta s_z s_\theta)\dot{\epsilon}_\theta + ((\alpha+1) - \beta s_z^2)\dot{\epsilon}_z - \beta s_z s_{rz}\dot{\gamma}_{rz}],\\
\dot{\tau}_{rz} &= 2\mu[-\beta s_{rz} s_r \dot{\epsilon}_r - \beta s_{rz} s_\theta \dot{\epsilon}_\theta - \beta s_{rz} s_z \dot{\epsilon}_z + (1/2 - \beta s_{rz}^2)\dot{\gamma}_{rz}],
\end{aligned} \tag{1.6}$$

on $\mathscr{H}$ for $t > 0$: here s_r, s_θ, s_z, s_{rz} are the normalized stress deviators,

$$s_r = (2\sigma_r - \sigma_\theta - \sigma_z)/(3\sqrt{3}\tau_0), \quad s_\theta = (2\sigma_\theta - \sigma_z - \sigma_r)/(3\sqrt{3}\tau_0),$$
$$s_z = (2\sigma_z - \sigma_r - \sigma_\theta)/(3\sqrt{3}\tau_0), \quad s_{rz} = \tau_{rz}/(3\sqrt{3}\tau_0),$$

with τ_0 being the octahedral shear stress,

$$\tau_0 = (\sqrt{2}/3)(\sigma_r^2 + \sigma_\theta^2 + \sigma_z^2 - \sigma_\theta\sigma_z - \sigma_z\sigma_r - \sigma_r\sigma_\theta + 3\tau_{rz}^2)^{1/2},$$

and α, β are material constants,

$$\alpha = \nu/(1-2\nu), \quad \beta = \mu/(\mu + \mu_p),$$

†The usual notation for the stress and strain components is employed and u, w are the displacements in the r, z directions respectively; throughout, a dot atop a quantity indicates the corresponding rate.

with ν being Poisson's ratio, μ the shear modulus and μ_p the plastic octahedral shear modulus defined by $\mu_p = \dot{\tau}_0/2\dot{\epsilon}_0$, where $\dot{\epsilon}_0$ is the octahedral plastic strain rate, the analogue of $\dot{\tau}_0$. The *strain-rate/displacement-rate relations* for infinitesimal strain rates,

$$\dot{\epsilon}_r = \frac{\partial \dot{u}}{\partial r}, \qquad \dot{\epsilon}_\theta = \frac{\dot{u}}{r},$$
$$\dot{\epsilon}_z = \frac{\partial \dot{w}}{\partial z}, \quad \dot{\gamma}_{rz} = \frac{\partial \dot{u}}{\partial z} + \frac{\partial \dot{w}}{\partial r}, \tag{1.7}$$

on $\mathscr{H}$ for $t > 0$. The *contact conditions* under the rigid sphere,

$$\dot{w} = \Delta w, \tag{1.8}$$

on $\partial_1\mathscr{H}$ for $t > 0$, wherein Δw is the prescribed rate of increase of w, constant throughout the contact region, in conjunction with either

$$\dot{u} = 0 \quad \text{or} \quad \dot{\tau}_{rz} = 0, \tag{1.9}$$

on $\partial_1\mathscr{H}$ for $t > 0$, the first modelling adhesive contact (slip completely restrained) while the second approximates lubricated contact (perfectly smooth). The *stress-free conditions* on the remainder of the half-space surface,

$$\dot{\sigma}_z = \dot{\tau}_{rz} = 0, \tag{1.10}$$

on $\partial_2\mathscr{H}$ for $t > 0$. And, finally, the *conditions at infinity* which take the displacements to remain zero there,

$$\dot{u} = o(1), \ \dot{w} = o(1) \text{ as } r^2 + z^2 \to \infty, \tag{1.11}$$

on $\mathscr{H}$.

Several comments concerning the modelling underlying the problem class formulated are in order. First, the quasi-static response of a half-space can be physically representative of the *dynamic* indentation of *finite* targets when their extent is an order of magnitude greater than the ultimate contact radius induced, yet the duration of indentation is an order of magnitude longer than the time taken for the leading elastic wavefront to traverse the target.† In practice it is somewhat surprising how many apparently highly transient situations comply with these requirements and are therefore amenable to treatment as quasi-static. Second, the usual inverse approach is adopted to overcome the geometric non-linearity caused by the conforming contact, that of not knowing the contact radius *a priori* for a given load; thus a, $\dot{a}$ are in effect set in (1.8) via prescription of $\partial_1\mathscr{H}$ and P backed out. Third, an approximation, reasonable for $a^2/R^2 \ll 1$, is involved in the lubricated instance in (1.8), (1.9) where cylindrical coordinates are used instead of the local spherical coordinates needed for an exact, but less tractable, statement. The intent of the different contact conditions in (1.9) is to bound the effects of *friction*. Last, the simplification of a *rigid* spherical indenter is appropriate when the response of the indented half-space is of concern rather than that of the indenter, and is realistic for actual configurations in which the indenter experiences relatively little total—elastic plus plastic—deformation. That is, in instances in which there is significant plastic flow, when the indenter is sufficiently relatively hard so as not to yield appreciably.

Turning to the nature of the problem class at hand, we note that the quasi-static assumption means that, although relationships change with time, they are independent of the time scale. Hence, in essence, we are faced with solving for the ten rate, or incremental, quantities in $\dot{\sigma}$, $\dot{\epsilon}$, $\dot{u}$, as functions of the two variables r, z, satisfying the quasi-linear system

†This is basically an adaptation of Love's criterion ([13], Section 139).

of partial differential equations (1.5)–(1.7) together with the conditions (1.8)–(1.11)—a task almost certainly intractable to any purely analytical approach. Accordingly we look to numerical solution methods in what follows and, to this end, require the specification of the requisite material constants for a particular problem before proceeding further. For the purposes of this paper a single material for experimental comparison suffices, the actual material chosen being 304L stainless steel. Thus $\nu = 0.28$, $\mu = 10.9 \times 10^3$ ksi (75.4×10^3 MPa) and μ_p is provided in effect by the stress-strain curve (Fig. 2). Implicit in the definition of μ_p is a limiting value of τ_0 which heralds the onset of plastic flow; initially this is the octahedral yield stress $\tau_y = 16.6$ ksi (115 MPa), but as the material work hardens this quantity is updated to take on the value attained locally in accordance with the stress-strain curve. With these details now in place we next move on to the solution technique to be used.

2. ANALYSIS

In this section we consider the application of an elasto-plastic, finite element code to the contact problem of interest, beginning with a discussion of element selection and arrangement, continuing with a description of the procedure used to track the indentation which includes a simple yet effective expansion technique, and closing with a summary of the calculations performed.

The quasi-linear nature of the governing equations in the preceding formulation enables an energy principle—the analogue of the principle of minimum potential energy in elasticity—to be established for the incremental field quantities of elasto-plastic flow. This principle forms a natural basis for finite element methods (FEM) and several codes exist which implement this type of FEM (see, e.g. [14]). Underlying the approach in these codes is the discretization of the continuum involved and a number of elements for this purpose are available. Basically the performance of the various elements can be classified in the following manner: with a constant approximation to the stress field throughout an element the errors in the stresses decay as $O(h)$, where h is a lineal measure of element size, provided the stresses themselves are continuous; with a complete linear representation of the stresses in an element the errors decay as $O(h^2)$ provided the stresses together with their first derivatives are continuous; with a complete quadratic representation errors decay as $O(h^3)$ provided the stresses are twice continuously differentiable; and so on.† In general, the smoother the problem the more advantageous it is to employ higher-order elements. However, if a high-order element is used on a problem which does not meet its continuity requirement then not only can convergence be below the normal rate of that element, but

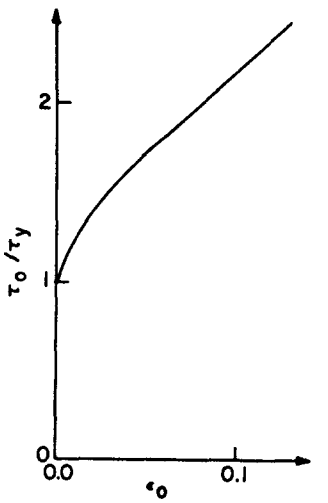

Fig. 2. Octahedral stress-strain curve for 304L stainless steel

†A more detailed account of element convergence may be found in [15], Section 2.2.

it can also be below the rate normally achieved with a lower-order element. Consequently we let the expected continuity in our problem dictate the element to be used.

In the initial stages of indentation our lubricated contact problem is elastic so that Hertz's solution [8] applies and shows that the only loss of continuity occurs at the edge of the contact region where $\sigma = O(\delta^\lambda)$ as $\delta \to 0$, $\delta = \sqrt{(r-a)^2 + z^2}$, with $\lambda = 1/2$. Hence the stresses there are continuous but not continuously differentiable and the situation cannot be expected to improve for the adhesive contact problem. Moreover, while it is not known precisely how this behavior is modified by the presence of plastic flow, studies, such as those performed by Hutchinson[16], Rice and Rosengren[17], indicate that λ probably decreases but only slightly, so that it seems likely that the first derivatives of the stress field remain discontinuous. As a result we choose the *axisymmetric, constant-stress triangle* as the element for the present problem.

To discretize the half-space using these elements we first exploit the axisymmetry of the problem to confine attention to a quarter-plane, say

$$\mathcal{Q} = \{(r, \theta, z) | 0 < r < \infty, \theta = 0, 0 < z < \infty\}. \tag{2.1}$$

Each triangular element within this region really represents a hoop of triangular cross-section, points in which maintain a fixed distance from the z-axis. Next we must limit the extent of $\mathcal{Q}$ to be discretized. Since it is reasonable to expect material remote from the contact region not to yield and, by Saint-Venant's principle, to be influenced for the most part by the load P, it is to be anticipated from the Boussinesq solution that the stresses go to zero in accordance with $O(Pa^2/\rho^2)$, the displacements in accordance with $O(Pa/\rho)$, as $\rho/a \to \infty$, $\rho = \sqrt{r^2 + z^2}$. Hence, because resolution to within about 1% certainly suffices for most engineering purposes, we restrict discretization on $\mathcal{Q}$ to a quadrant of a circle of radius $A \sim 100a$. Within this quadrant some graduation of element sizes is desirable in order to efficiently capture the variations present. As field quantities are generally smoother once plastic flow has started, we again draw on Hertz's elastic solution [8] to provide what are probably the most severe gradients and adjust the grid refinement so that the element-to-element changes in the elastic stresses are approximately equal. There is, in addition, a need while constructing this non-uniform grid to maintain *locally isotropic* arrangements of the elements since the material being modelled is itself isotropic, i.e. to generate repeating, similar, element patterns with nodes which see nearly the same element distribution in all directions. And finally, there is a need to place as many nodes in the contact region as possible since, when each node is brought into contact as indentation proceeds, the half-space experiences an apparent sudden jump in contact extent giving rise to an artificial unloading, and it is desirable to keep these non-physical byproducts of the discretization as small as possible.† These last considerations are somewhat at variance with designing a grid or map which entails a reasonable level of computational effort; the compromise arrived at is shown in Fig. 3 wherein the map has 497 elements and 287 nodes or 574 degrees of freedom, features nodes alternately at the centers of "union jacks" or "kites" throughout most of the inner critical region, and has additional refinement in the contact region.

We take the conditions on the outer circular boundary of the grid to be

$$\dot{w} = 0, \ \dot{T}_r = 0, \tag{2.2}$$

on $\mathcal{Q}$ for $\rho = A$, where T_r is the traction in the radial direction. The first of (2.2) reflects the latter infinity condition of (1.11) and assures the existence of self-equilibrating nodal forces in the z-direction. The second of (2.2) is a departure from the most obvious, namely

†In fact failure to preserve a grid with an almost periodic, self-similar, isotropic arrangement and sufficient refinement in the contact region resulted, in an early attempt at an FEM analysis of the present problem, in extraneous element-to-element fluctuations to such an extent that the element stresses were rendered physically meaningless at quite moderate load levels even though the elastic solution was accurately reproduced initially. We do not completely understand the source of such numerical noise at this time and a fuller appreciation of how best to alleviate it is a subject of ongoing research.

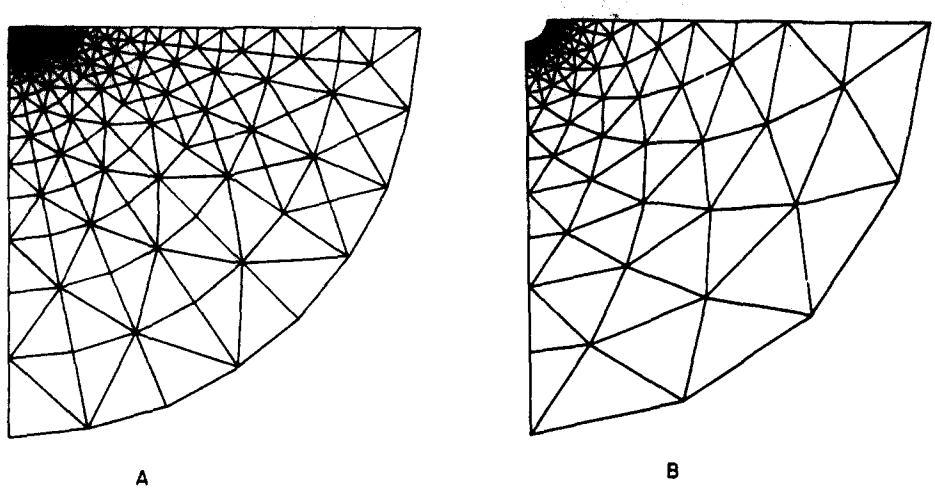

Fig. 3. Finite element grid: (A) Inner region; (B) Outer region

$\dot{u} = 0$, so as to avoid the introduction of spurious singularities at the intersection of the circular boundary with the upper free surface. Along the upper surface the stress-free conditions (1.10) are enforced outside the contact region ($a < r < A$, $z = 0$) while one of the contact conditions of (1.8), (1.9) is enforced within the contact region ($0 < r < a$, $z = 0$). On the remaining straight boundary symmetry conditions are applied, *viz.*

$$\dot{u} = 0, \ \dot{\tau}_{rz} = 0, \tag{2.3}$$

on $r = 0$, $0 < z < A$.

Of course the contact region on which (1.8), (1.9) are applied is not constant; however, the FEM solution algorithm calls for incremental loading and this incremental nature facilitates handling the expanding contact area. If, for a given load increment, the accumulated displacement w of the first node outside the current contact region is computed to be less than the displacement of the corresponding location on the rigid sphere, then the contact area is enlarged to include this node and the load increment recomputed.

The specifics of how loads are increased are as follows. The initial indentation is adjusted so as to just induce yielding in a single element. Actually this first load step represents the accumulation of a number of steps satisfying (1.8) which, since the problem is linear in the elastic state, can be applied directly in a single step by setting

$$w = (2a^2 - r^2)/2R, \tag{2.4}$$

on $z = 0$, $0 < r < a$. Thereafter the indentation diameter is successively increased by $2\frac{1}{2}\%$, that is, $\dot{a} = 0.025a$ so that $\dot{a}$ itself increases. When the contact area expands to the point of including a further node, $\dot{a}$ is reset to its original level and the new node brought into contact more gradually so as to reduce numerical noise. The process is then repeated to bring in the next node, and so on.

As indentation proceeds our FEM grid in effect shrinks, its radius A no longer remains of the order of $100a$, and the degree to which (2.2) reflects the infinity conditions becomes an issue. Further, while the greatest field gradients are initially being tracked by the inner smaller elements, as yielding proceeds the fields represented by these elements become relatively uniform and the steepest gradients radiate out to the coarser elements—potentially an inefficient discretization. To avoid these shortcomings we employ a straightforward *expansion technique* which is most readily viewed as a periodic scaling up of the map so that it returns to its original extent of approximately $100a$. In actuality there is no need to alter the grid size, but merely to transfer field quantities back to their corresponding points. The quantities transferred are the element stress and strain

components, the nodal displacements and forces, the element, octahedral, plastic stresses, strains and moduli, the plastic work in the elements, and reference octahedral stress values (equal to the octahedral yield stress for unyielded elements, the present value for elements currently undergoing plastic flow, and the highest previous value for elements currently unloading elastically). The self-similar nature of the grid refinement aids transfer, many of the original exterior elements simply assuming the identity of an interior element. An interpolation procedure is required for those "post-expansion" elements which do not coincide exactly with an original element but rather take on the information contained by a number of elements. Consistent with the approximation implicit in axisymmetric constant-stress elements we choose a scheme which reduces to linear interpolation in simple instances and which recognizes the volume truly represented by elements (see [18], Appendix 1 for details). Those post-expansion exterior elements and nodes which have no counterparts prior to expansion are taken to be in the virgin state. The actual point at which rescaling is undertaken is when the contact region has grown to 2.4 times its initial radius. For the analysis at hand, implementation of this expansion technique lead to a reduction in computation time of an order of magnitude without loss of resolution.

Using the foregoing approach a number of calculations can be examined with a view to validating the analysis. An obvious one is to compare the initial elastic load step for the lubricated case with Hertz's solution [8]. For this step too, the expansion technique can be prematurely applied to furnish a sequence of grids in effect and thus enable convergence to be examined. As plastic flow commences, though, no elasto-plastic exact solution appears to be available for checking against. Nonetheless, by setting $\dot{a}$ equal to $0.05a$, $0.025a$, $0.0125a$, convergence with load increment can be considered, and by performing the calculations with the real material values for 304L stainless steel comparison with a companion set of experiments can be made. This last set of calculations is undertaken for both contact conditions and entails computation for a large number of increments (~ 5000) with computational effort for a single contact condition running at the level of approx. 20 hr CPU time on the DEC-20 system at Carnegie-Mellon University. We next review the results of performing such calculations.

3. VERIFICATION

Here we check the numerical convergence of our approach—spatially, for the first load step, against the elastic solution and temporally for varying load increments— then describe a set of experiments which enable the force/indentation predictive capability of the analysis to be assessed at high load levels of the order of 10^5 times the load at yield.

For the grid of Fig. 3, the first, elastic, load step brings 14 nodes into contact. By expanding for this load step, maps which have 8 and 5 nodes in contact can be generated and this device thereby provides a geometrically similar sequence of a fine, a medium, and a coarse map to evaluate convergence on. Since Hertz's solution [8] is available for elastic lubricated contact we examine the stresses associated with this contact condition for convergence—stresses rather than displacements because the former are more critical from a convergence point of view. For all three grids, the normal stress component σ_z on the z-axis is calculated at the nodes there by averaging surrounding elemental values and compared with the exact result from Huber[19] after Hertz[8] of

$$\sigma_z/\sigma_o = 1/(1 + z^2/a^2), \tag{3.1}$$

on $r = 0$ for $0 \leq z < \infty$, where $\sigma_o = -3P/2\pi a^2$ is the contact pressure under the center of the sphere. The results (Fig. 4) are consistent with a numerically convergent scheme and demonstrate that the "fine" grid, the one to be used to take calculations forward, has good resolution.

A more stringent convergence test obtains if we consider the contact pressure, σ_z on $\partial_1\mathscr{H}$. Here element values have to be extrapolated to the surface in contrast to on the z-axis where complete clusters of elements surround nodes by virtue of the axisymmetry. The extrapolation procedure incurs numerical noise which we smooth with a least squares fit

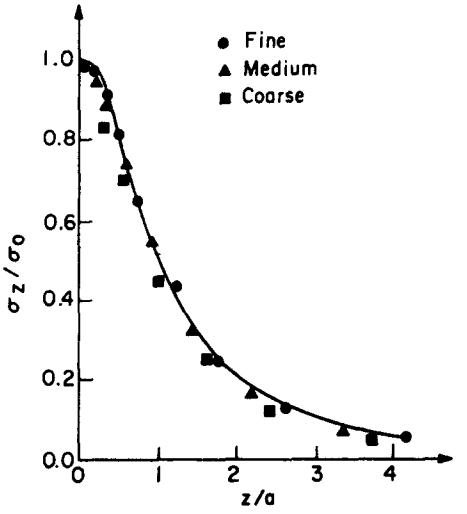

Fig. 4. FEM convergence for the elastic stress σ_z down the z-axis

of

$$\sigma_z = (c_1 + c_2 r^2 + c_3 r^3 + c_4 r^4)\sqrt{1 - r^2/a^2}, \tag{3.2}$$

on $\partial_1\mathscr{H}$, $c_i (i = 1 - 4)$ being the fitted constants. Applying (3.2) to the stresses from all three grids then allows comparison with the exact expression from Hertz[8],

$$\sigma_z/\sigma_o = \sqrt{1 - r^2/a^2}, \tag{3.3}$$

on $\partial_1\mathscr{H}$. The results (Fig. 5) are again in accord with numerical convergence and indicate that adequate accuracy is furnished by the grid for ultimate use.

One means of quantifying the convergence shown in Figs. 4 and 5 is to model the error distribution e by

$$e = e_o h^c, \tag{3.4}$$

wherein h is an average lineal measure of grid size in the region common to all three grids, e_o is the error for unit h, and the exponent c reflects the *rate of convergence*. Applying (3.4) to the stress results in Figs. 4 and 5 yields

$$0.75 < c < 1.25. \tag{3.5}$$

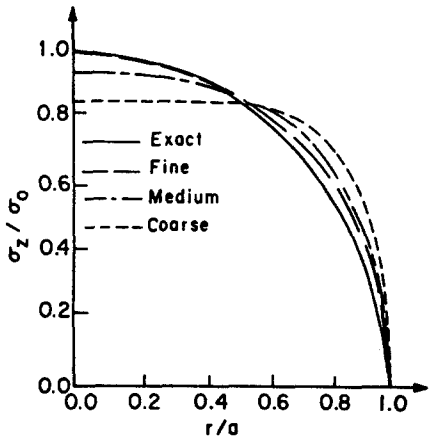

Fig. 5. FEM convergence for the elastic contact pressure

Hence the convergence is in fair agreement with that expected of constant stress elements ($c \to 1$ as $h \to 0$).

Convergence with load increment is likewise satisfactory: after 14 load steps the stress responses throughout the half-space altered by less than 0.1% on reducing $\dot{a}$ from $0.05a$ to $0.025a$, and by less than 0.01% on further reducing $\dot{a}$ to $0.0125a$. As a result $\dot{a}$ was set at $0.025a$ for the remainder of the calculations.

In view of the apparent lack of any analytical solutions for our contact problem within the context of incremental elasto–plasticity once yielding commences, we look to a set of experiments to provide a check on our analysis in this instance. The set of experiments involves simple indentation tests using a commercially-available, Rockwell, hardness, test apparatus. In the hardness tests a 1/16 in. (1.59 mm) diameter, spherical indenter made of high-strength tool steel is forced slowly into smooth flat substrates of annealed 304L stainless steel under controlled normal loads of 33, 66 and 99 lbf (147, 294, 441 N). The diameters of the indentations produced under these loads are readily measured with a travelling microscope (*cf.* the depths of indentation), two orthogonal measurements being made on each indentation. No fewer than 10 indentations are made and measured at each load; Fig. 6 displays the average values so obtained together with horizontal bars which represent ranges of $\pm 2s$, s being the standard deviation.

Since the indented material is considerably softer than the indenter the experimental situation approximates the contact problem of interest well and the FEM analysis can be expected to predict the experimental measurements. Also shown in Fig. 6 therefore are the results of FEM analyses for both the adhesive and the lubricated contact conditions. Generally there is little difference between the two contact conditions although the adhesive condition does appear to promote more numerical noise. This similarity would seem physically reasonable since the spherical indenter tends to produce deformation normal to its surface rather than parallel to, so that friction effects play a minor role. As a consequence of the closeness of the two, only the lubricated condition calculations were taken out to the upper load levels which correspond to of the order of 10^5 times the load at yield, P_y.† At these high loads levels the approximation underlying the smooth contact conditions, namely $a^2/R^2 \ll 1$, is certainly starting to break down. Even so the FEM predictions track the physically observed response well.

The performance of the FEM analysis with respect to both the convergence checks and

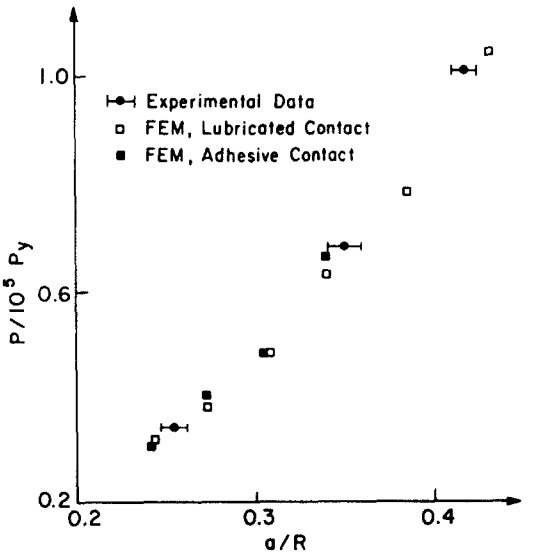

Fig. 6. Comparison of FEM predictions with measured indentation diameters in hardness tests

†The load at yield P_y can be estimated from the elastic solution (Huber[19]) by assembling τ_0 from expressions therein and setting it equal to τ_y; for our particular experimental configuration this gives $P_y = 9.6 \times 10^{-4}$ lbf (4.3×10^{-3} N).

the experimental verification support its use to determine further quantities of interest. The extensive results attending such an investigation are planned for presentation in the second part of this study.

Acknowledgements—We are pleased to extend our thanks to J. Lewandowski of the Department of Metallurgical Engineering and Materials Science at Carnegie-Mellon University, for his careful performance of the stainless steel experiments, and to J. L. Swedlow of the Department of Mechanical Engineering, C-M.U., for some helpful comments on the use of his finite element code. The financial support of the Department of Energy under grant number DE-AC02-79ER10468 is also appreciated.

REFERENCES

1. J. J. Kalker, A survey of the mechanics of contact between solid bodies. *Z. Angew. Math. Mech.* **57**, T3 (1977).
2. G. E. Dieter, *Mechanical Metallurgy*, 2nd Edn. McGraw-Hill, New York (1976).
3. J. C. Tyler, R. A. Burton and P. M. Ku, Contact fatigue under oscillatory normal load. *Trans. Am. Soc. Lubric. Engrs* **6**, 255 (1963).
4. P. S. Follansbee, G. B. Sinclair and J. C. Williams, Modelling of low velocity particulate erosion in ductile materials by spherical particles. *Wear* **74**, 107 (1981).
5. J. O. Almen and P. H. Black, *Residual Stresses and Fatigue in Metals*. McGraw-Hill, New York (1963).
6. D. Tabor, *The Hardness of Metals*. Oxford at the Clarendon Press (1951).
7. K. L. Johnson, Inelastic contact: plastic flow and shakedown. *Proc. Int. Symp. on Contact Mechanisms and Wear of Rail-Wheel Systems*, Vancouver (1982).
8. H. R. Hertz, *Miscellaneous Papers*. English transl., Macmillan, London (1896).
9. A. J. Ishlinsky, The axi-symmetrical problem in plasticity and the Brinnel test. *Prikl. Mat. Mekh.* **8**, 233 (1944).
10. R. T. Shield, On the plastic flow of metals under conditions of axial symmetry. *Proc. R. Soc.* (Lond.) **A233**, 267 (1955).
11. C. Hardy, C. N. Baronet and G. V. Tordion, The elasto–plastic indentation of a half-space by a rigid sphere. *Int. J. Num. Meth. Engng* **3**, 451 (1971).
12. C. H. Lee, S. Masaki and S. Kobayashi, Analysis of ball indentation. *Int. J. Mech. Sci.* **14**, 417 (1972).
13. A. E. H. Love, *A Treatise on the Mathematical Theory of Elasticity*, 4th Edn. Dover, New York (1944).
14. J. L. Swedlow, A procedure for solving problems of elasto–plastic flow. *Comput. Structures* **3**, 879 (1973).
15. G. Strang and G. F. Fix, *An Analysis of the Finite Element Method*. Prentice-Hall, New Jersey (1973).
16. J. W. Hutchinson, Singular behaviour at the end of a tensile crack in a hardening material. *J. Mech. Phys. Solids* **16**, 13 (1968).
17. J. R. Rice and G. F. Rosengren, Plane strain deformation near a crack tip in a power hardening material. *J. Mech. Phys. Solids* **16**, 1 (1968).
18. P. S. Follansbee, Mechanisms of erosive wear of ductile metals due to the low velocity, normal incidence, impact of spherical particles. Ph.D. Dissertation, Carnegie-Mellon University, Pittsburgh (1981).
19. H. T. Huber, Stresses in the contact of two elastic spheres. *Annls Phys.* **14**, 153 (1904).